Nanoscale

Accepted Manuscript

This article can be cited before page numbers have been issued, to do this please use: J. Zhang, X. Yu, W. Guo, J. Qiu, X. Mou, A. Li and H. Liu, *Nanoscale*, 2016, DOI: 10.1039/C6NR01360K.

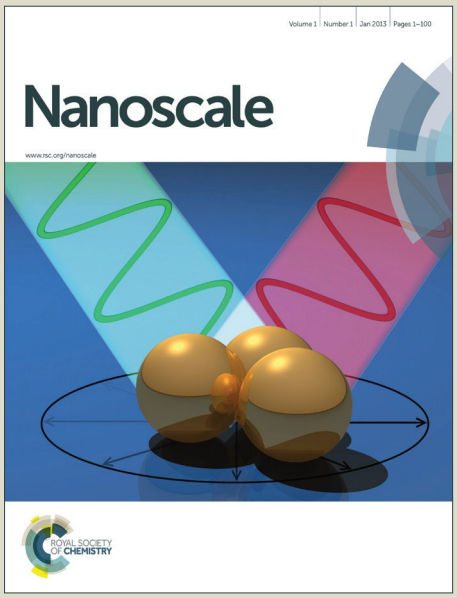

ROYAL SOCIETY OF CHEMISTRY

www.rsc.org/nanoscale

View Article Online
DOI: 10.1039/C6NR01360K

Construction of titanium dioxide nanorod/graphite microfiber hybrid electrodes for high performance electrochemical glucose biosensor

Jian Zhang,[a,1] Xin Yu,[a,1] Weibo Guo,[1] Jichuan Qiu,[1,2] Xiaoning Mou,[1] Aixue Li,*[3] Hong Liu*[1,2]

1Beijing Institute of Nanoenergy and Nanosystems, Chinese Academy of Sciences; National Center for Nanoscience and Technology (NCNST), Beijing, 100083, P. R. China.

2 State Key Laboratory of Crystal Materials, Shandong University, Jinan, 250100, P. R. China.

3 National Research Center of Intelligent Equipment for Agriculture, Beijing Academy of Agriculture and Forestry Sciences, Beijing, 100097, China.

a These authors contributed equally to this work.

E-mail: hongliu@sdu.edu.cn, lax200178@aliyun.com

Abstract: The demand for a highly sensitive and selective glucose biosensor which can be used for implantable or on-time monitoring is constantly increasing. In this work, TiO_2 nanorods were synthesized in situ on the surface of graphite microfibers to yield TiO_2 nanorod/graphite microfiber hybrid electrodes. The TiO_2 nanorods not only retain the high activity of the immobilized glucose molecule, but also promote the direct electron transfer process on the electrode surface. As a working electrode in an electrochemical glucose biosensor in a flowing system, the microfiber hybrid electrodes exhibit high sensitivity, selectivity and stability. Due to its simple, low cost, high stability, and unique morphology, the TiO_2 nanorod/graphite microfiber hybrid electrode is expected to be an excellent candidate for an implantable biosensor or for in situ flowing monitoring.

1. Introduction

Fast, convenient and reliable determination of glucose plays a crucial role in various fields including food, biofuel cells, textile industry, health and medical system.[1,2] To date, various detection methods have been proposed to develop sensitive and selective glucose sensors.[3,4] Among these methods, electrochemical methods based on enzymatic glucose oxidation are currently one category of the most active methods.[1,5] As an ideal mode enzyme, glucose oxidase (GOx) has been widely used in electrochemical glucose biosensors due to its high reactivity and selectivity for glucose recognition.[6,7] Unfortunately, the redox center of the enzyme is usually seated deeply in a thick insulating protein shell. The spacing between the prosthetic group of GOx and the sensing surface generally exceeds the critical electron-tunneling distance. Therefore, the direct electron transfer (DET) between the flavin adenine dinucleotide (FAD) of GOx and the bare electrode surface is difficult. Usually, the electron mediators are employed to facilitate DET process.[8-10]

TiO_2, a metal oxide semiconductor, has been attracted considerable interest in biosensor because of its high conductivity, good biocompatibility and large surface area.[9,14-19] It has been found that TiO_2 could promote the interaction between GOx and electrode surface and facilitate the DET reaction due to its large surface area and improved electron transfer rate.[21,22] Therefore, several enzymatic glucose biosensors based on TiO_2 nanoparticle assembled electrodes have been developed.[9,20] However, in most cases, TiO_2 nanoparticle electrode is built by coating a layer of mixture of TiO_2 nanoparticle-conductive organic molecules or conductive adhesive on the surface of the glassy carbon (GC) electrode.[9,20,23] This kind of electrodes have several disadvantages, which is the great obstacle for their practical application as biosensors. The first disadvantage is the adhesive organics often block some active facets of TiO_2

View Article Online
DOI: 10.1039/C6NR01360K

nanoparticles, which should lower the activity. The second one is the TiO_2 active layer is easily to exfoliate during the detection process in the solution, causing lower stability. In addition, large amount of boundary with the bonding materials among the nanoparticles could reduce the electron transfer speed from active sites to the electrode surface. Therefore, building novel TiO_2-based biosensors with high electrochemical active area and stability for a significant improvement in glucose sensing is still a great challenge.

So far, there have been some reports about the in situ synthesis of TiO_2 on various substrates, including Si wafers, titanium metal plates, carbon cloth as well as conductive glass slides, which have been used in biosensors or photoelectric devices.[10,24-26] These kinds of electrodes have solved the electron transfer problem and the problem of exfoliation of the active layer. However, the limited active site because of the 2D electrode and the rigidity of the hard substrates still limit their applications. More recently, carbon or graphite microfiber electrodes have attracted much attention because of their special one-dimensional morphology, small size and high conductivity. When nanostructures are formed on the flexible carbon or graphite microfiber, the functional hybrid electrode will possess large electrochemical active surface area, high utilization efficiency of active materials, and superior electron transport property compared with common solid electrodes.[27-29] In addition, these kinds of hybrid electrode will have the potential to be used in vivo. Nowadays, the carbon microfiber-supported TiO_2 nanomaterials have been applied in the fields of solar cells and photocatalysis systems.[30-32] However, to our knowledge, there are few report about its application in the field of electrochemical biosensors. Graphite microfiber is carbon-based microfiber with graphitization degree over 95%. Their chemical and physical stability, flexibility, and conductivity are much better than carbon microfiber.

In this work, we synthesized TiO_2 nanorods in situ on surface of graphite microfiber through a hydrothermal method, and formed a TiO_2 nanorod/ graphene microfiber hybrid material. The TiO_2nanorods are vertically grown on the surface of the graphite microfibers directly. For the first time, a fibroid glucose biosensor with high performance in a flowing system was constructed by immobilizing GOx onto the hybrid microfiber by using natural biopolymer, chitosan as connection molecules. This kind of electrode was proved to be a perfect glucose biosensor with high sensitivity and high selectivity because of its three dimensional structure, more active facets, and fast direct electron transfer property. Because this TiO_2-based graphite microfiber electrode can be used to detect various biomolecules in vitro or in vivo, we envision that it will become an important platform for building various electrochemical biosensors.

2. Results and discussion

2.1 Characterization of TiO_2 nanorod/graphite hybrid microfiber enzyme electrode

View Article Online
DOI: 10.1039/C6NR01360K

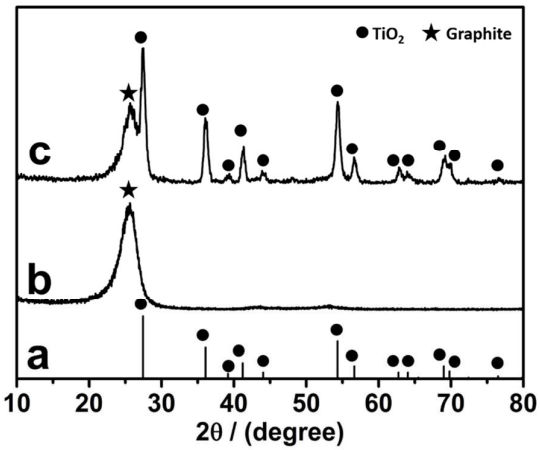

Figure 1. XRD patterns of (a) TiO_2 JCPDS no. 21-1276, (b) graphite microfiber, (c) TiO_2 nanorod/graphite microfiber

X-ray powder diffraction (XRD) was used to determine the crystalline phase of the graphite microfiber and the hybrid microfiber, as shown in Figure 1. The diffraction peak centered at 2θ=25.728 of the graphite microfiber (Figure 1b) can be indexed as graphite without any other peak of second phase (JCPDS no. 65-6212), which indicates that the microfiber is high purity graphite. The crystalline phase of the hybrid microfiber was shown in Figure 1c. Beside the peak of graphite, all other peaks are consistent with the standard diffraction peaks of tetragonal rutile TiO_2 (JCPDS no. 21-1276, Figure 1 a). This result indicates that graphite crystalline phase has not changed in the hybrid microfiber, while new rutile TiO2 phase appears.

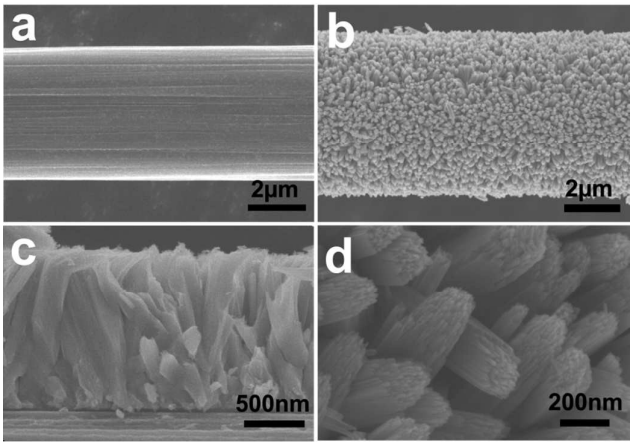

Figure 2. SEM images of graphite microfiber (a), TiO_2 nanorod/graphite microfiber (b and c) and high resolution images of TiO_2 nanorods on the surface of graphite microfiber

The morphology of the as-prepared TiO_2 nanorod/graphite hybrid microfiber was characterized by scanning electron microscopy (SEM), as shown in Figure 2. The commercial graphite microfibers have smooth surface with some stripes formed during the stretch forming process, and the diameter is about 5-6μm, as shown in Figure 2a and Figure S1a. SEM image of TiO_2 nanorod/graphite hybrid microfiber shows the graphite microfiber is densely covered with a layer of TiO_2 nanorods with uniform size (Figure 2b). From the split part of the hybrid microfiber, as shown in Figure 2c, we can see that the TiO_2 nanorods vertically grown on the surface of graphite microfiber tightly, and the length of TiO_2 nanorods

View Article Online
DOI: 10.1039/C6NR01360K

is about 1.1μm. The high resolution image of the TiO_2nanorods shows that the nanorods are tetragonal prisms with diameters of 150-200nm, as shown in Figure 2d. More detailed observation indicates that the tetragonal prisms are assembled by very small nanowires with diameter about 20nm. This special nanostructure ensure a large number of active facets can be used as sensitive sites.

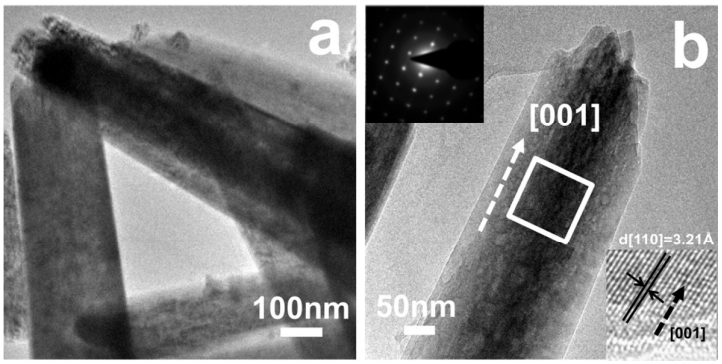

Figure 3. TEM images of TiO_2 nanorods (a), and high resolution images of TiO_2 nanorods (insets of SAED and HRTEM) (b).

Figure 3 shows the typical transmission electron microscopic (TEM) images of TiO_2 nanorods from the surface of the TiO_2 nanorods/graphite microfiber. Figure 3a shows that the diameter of the nanorods are about 150-200nm, which is consistent with the results from SEM images. Figure 3b exhibits the single-crystalline nature of these nanorods, which is verified with the selected area electron diffraction (SAED) pattern. The inset of the HRTEM image shows One set of the lattice spacings is about 0.321nm, corresponding to the [001] crystal orientation of rutile TiO_2 which is orthogonal to the surface of the graphite microfiber.[33] Figure S1 shows more information about the characterization of TiO_2 nanorods/graphite microfiber hybrid nanostructures. During the hydrothermal process, all the graphite microfibers can be assembled with TiO_2 nanorod uniformly. Based this kind of TiO_2 nanorods/graphite microfiber bundle, a three dimensional electrode can be obtained.

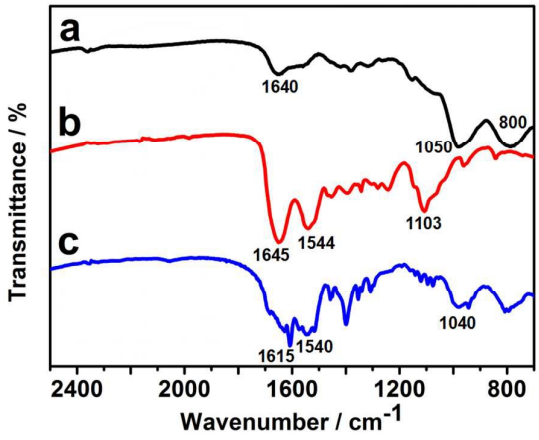

Figure 4. FTIR spectra of (a) chitosan/TiO_2 nanorod/graphite microfiber, (b) GOx and(c) GOx/chitosan/TiO_2 nanorod/graphite microfiber.

The immobilization of GOx protein on TiO_2 nanorod/graphite microfiber electrode was investigated by Fourier-transformed infrared (FTIR) spectroscopy, as shown in Figure 4. For the chitosan/TiO_2 nanorod/graphite microfiber (Spectrum a), the remarkable peak at 800cm^{-1} corresponds to the bending

View Article Online
DOI: 10.1039/C6NR01360K

vibrational mode of Ti-O-Ti bonds. Two peaks at 1640cm^{-1} and 1050cm^{-1}, which corresponds to the deformation vibration of H-O-H bonds and to the stretching vibration of Ti-O-C bonds respectively, also appear in the spectra of chitosan/TiO_2nanorods/graphite microfiber.[20,35] The spectrum for pure GOx molecules (Spectrum b) exhibit two characteristic peaks at 1645cm^{-1} and 1544cm^{-1}, which is ascribe to the typical amide I and amide II adsorption bands of the enzyme. The peak at 1103cm^{-1} is attributed to the C-O bond stretching vibration of GOx.[34] The spectra of GOx/chitosan/TiO_2 nanorod/graphite microfiber is shown in Spectrum c. It can been found that both the characteristic peaks of GOx (amide I and amide II bands) and TiO_2 (Ti-O-Ti bonds) can be observed. The amide adsorption peaks are shifted slightly to 1615 and 1540 cm^{-1}, and a shift of the Ti-O-C adsorption peak to 1040 cm^{-1} is also observed. It is possibly due to the strong electrostatic interaction between the negatively charged GOx and the positively charged TiO_2.[34,36,37] The FTIR results indicate that GOx is successfully immobilized on the TiO_2 nanorod/graphite microfiber and their secondary structure is retained after immobilization.

Electrochemical impedance spectroscopy (EIS) is an efficient method to investigate the charge transfer process at the electrode surface accompanying the stepwise modification. In fact, the charge transfer process is strongly influenced by any electrode surface modification. Especially the R_{ct} represents the resistance for charge transfer at the electrode surface. Figure S2A shows the Nyquist plots obtained with different microfiber electrodes in the presence of $K_3[Fe(CN)_6]/K_4[Fe(CN)_6]$ mixture. It can be obtained that the R_{ct} value of the chitosan/TiO_2 nanorod/graphite microfiber (curve b) is larger than that of the TiO_2nanorod/graphite microfiber (curve c), demonstrating that a layer of chitosan film is formed on the surface of microfiber electrode and blocked the electrode transfer between the redox probe and the electrodes. After the GOx molecules were immobilized on the chitosan/TiO_2 nanorod/graphite microfiber electrode surface, the R_{ct} value was further increased (curve a), indicating that the immobilization of GOx caused an inhibition of the electron transfer of redox couple to the electrode surface.[17,38] Cyclic Voltammetry (CV) result is shown in Figure S2B. After the layer by layer immobilization of chitosan and GOx, the current intensity is decreased and peak-to-peak separation between the anodic and cathodic waves is increased, indicating a weakened electron transfer process, which consistent with the result of EIS. The results of EIS and CV suggest the successful immobilization of chitosan and GOx film on the surface of TiO_2nanorod/graphite microfiber electrode.

2.2 Direct electrochemistry of GOx/chitosan/TiO_2 nanorod/graphite microfiber electrode

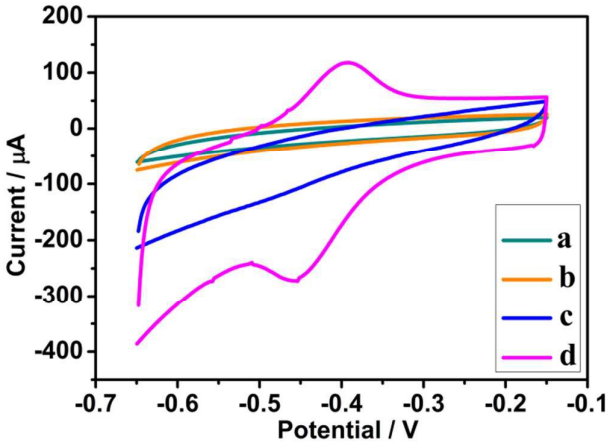

Figure 5. CV of (a) chitosan/graphite microfiber, (b) GOx/chitosan/graphite microfiber, (c) chitosan/TiO_2 nanorod/graphite microfiber and (d) GOx/chitosan/TiO_2 nanorod/graphite microfiber electrodes in 0.1 M

View Article Online
DOI: 10.1039/C6NR01360K

pH 7.0 N_2-saturated PBS at a scan rate of 50 mV s^{-1}.

To study the direct electron transfer of the GOx on the chitosan/TiO_2 nanorod/graphite microfiber electrode, CV measurements were performed in 0.1M N_2-saturated, phosphate buffered saline (PBS) solution (pH=7.0) at a scan rate of 50 mV s^{-1} (Figure 5). From CV curve of chitosan/ graphite microfiber electrode (curve a), GOx/chitosan/graphite microfiber electrode (curve b) and chitosan/TiO_2 nanorod/ graphite microfiber electrode (curve c), we can find no redox peak occurs on these three electrodes, indicating that both TiO_2 nanorods and GOx on graphite microfiber are electrochemically inactive at this circumstances. The background current of chitosan/TiO_2 nanorod/graphite microfiber electrode is higher than that of chitosan/graphite microfiber electrode and GOx/chitosan/graphite microfiber electrode, which is attributed to the large surface area of TiO_2 nanorods. However, two well-defined redox peaks are observed in the CV of the GOx/chitosan/TiO_2 nanorod/graphite microfiber (curved), indicating that GOx/chitosan/TiO_2 nanorod/graphite microfiber electrode could enable more effective electrical contact between redox active center of GOx and electrode surface, which is more suitable for the direct electrochemistry of GOx. The faster DET between the redox active site of GOx and microfiber electrode is according to the following equation (1), where FAD and FADH2 are the oxidized and reduced forms of the GOx redox center, respectively.

$$GOx\left(FAD\right)+2e^{-}+2H^{+}\leftrightarrow GOx\left(FADH_2\right)\ (1)$$

The influence of scan rate on the redox peaks current of the GOx/chitosan/TiO_2 nanorod/graphite microfiber electrode is also investigated in Figure S3a. It could be observed that with the increase of the scan rate, the redox potentials of GOx shifted slightly. The anodic current (I_{pa}) and cathodic peak current (I_{pc}) linearly increases linearly with the increasing scan rate from 30 to 200 mV s^{-1}, and the I_{pa}/I_{pc} ratio is approximately equal to 1 (Figure S3b). It indicates that the GOx redox reaction in GOx/chitosan/TiO_2 nanorod/graphite microfiber electrode is a quasi-reversible surface-controlled electrochemical process.[36,37]

The influence of the pH value on the electrochemical behavior of the GOx/chitosan/TiO_2 nanorod/ graphite microfiber electrode was also examined. As shown in Figure S4a, both the cathodic and anodic peak potentials shift negatively with an increase of solution pH value from 5.8 to 8.0. The redox peak potential as a function of the solution pH could be obtained from the following equation (2).

$$E=E^{0}+\frac{2.3RT}{nF}\log\left[\frac{C_{GOx(FAD)}\times\left(C_{H^2}\right)^2}{C_{GOx(FADH_2)}}\right](2)$$

The concentrations (C) of FAD and $FADH_2$ are constants in the electrochemical process, so the above equation could be simplified as the following equation (3) and (4).

$$E=E^{0}-\frac{2.3RT\times 2}{nF}pH\ (3)$$

$$E^{0'}=\text{constant}+0.059pH\ (4)$$

Where n, R, T and F are the number of transferred electrons, the gas constant, the temperature and the Faraday constant, respectively. The redox potentials change linearly as a function of the solution pH with a slope of -60.3mV pH^{-1} (Figure S4b). This slope is close to the theoretical value of -59mV pH^{-1}, indicating that two protons and two electrons are participated in the electron transfer process. In addition, the redox peaks current reach its maximum value at pH 7.0 (Figure S4c), possibly because the

View Article Online
DOI: 10.1039/C6NR01360K

GOx immobilized on the microfiber electrode has the highest bioactivity at a neutral pH. With an increase of pH, the peak current decreases, possibly due to the decrease of proton concentration and bioactivity of the GOx.[41,42] Hence, pH 7.0 PBS solution was used for further studies.

The surface coverage (Γ) of the enzyme molecules on the surface of the modified microfiber electrode can be estimated from the charge integration of the reduction peak at 50mV s^{-1} by the following equation (5).

$$\Gamma = Q / nFA \quad (5)$$

Where Q is the charge consumed in the reaction, n is the number of electrons being transferred, F is the Faraday's constant, and A is the electrode area. The surface coverage was calculated to be 2.518×10^{-9} mol cm^{-2}, which is larger than those of surface coverage at traditional modified GC electrode.[9,34,37,40] The large surface coverage may be resulted from the structure of the hybrid microfiber electrode.

The temperature was investigated for another important effect of response behavior of the GOx/chitosan/TiO_2 nanorod/graphite microfiber electrode, as shown in Figure S5. The current response increased while the temperature increased from 25 to 50°C, and then decreased while the temperature further increased. The maximum response appears at about 50°C. The current response decreased due to the denaturation of the enzyme at higher temperatures. However, in order to provide real applications conditions and convenient operating, 25°C was always chosen as the operating temperature for all further experiments.

2.3 Biosensor application

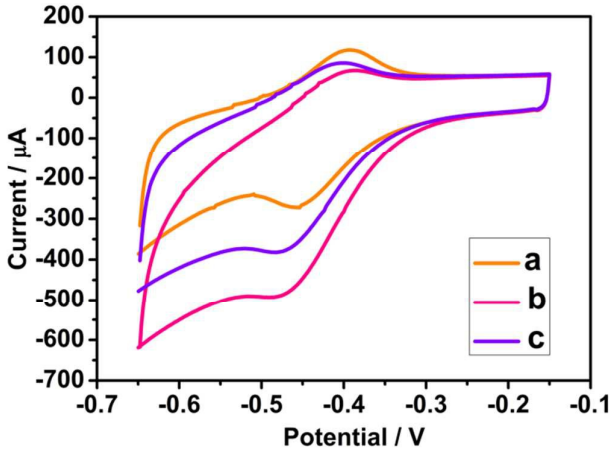

Figure 6. CV of GOx/chitosan/TiO_2 nanorod/graphite microfiber in 0.1 M pH 7.0 N_2-saturated PBS (a), O_2-saturated PBS (b), O_2-saturated PBS including 0.5 mM glucose (c) at a scan rate of 50mV s^{-1}.

CV measurements of the GOx/chitosan/TiO_2 nanorod/graphite microfiber electrode were carried out to study the glucose oxidation in N_2-and O_2-saturated pH 7.0 PBS in the absence and presence of glucose, as shown in Figure 6. As mentioned above, a pair of well-resolved redox peaks can be observed in N_2-saturated PBS (curve a). However, a great increase in reduction peak current and a simultaneous decrease in oxidation current could be clearly observed in O_2-saturated PBS (curve b), indicating a typical electrocatalytic process according to the equations (1) and (6).

$$GOx\left(FADH_2\right) + O_2 \rightarrow GOx\left(FAD\right) + H_2O_2 \quad (6)$$

View Article Online
DOI: 10.1039/C6NR01360K

In the presence of oxygen, the electrochemically formed GOx ($FADH_2$) electrocatalyzes the reduction of dissolved O_2, and the regenerated GOx (FAD) results in the loss of reversibility and an increase of the reduction peak current.[42,43] The enzymatic reaction of GOx with glucose is a first-order reaction.[44,45] As can be seen from curve c, when glucose was added into the O_2-saturated PBS, the reduction peak current decreased because the enzymatic reaction between the oxidized form of GOx (FAD) and glucose restrained the electrocatalytic reaction and reduced the concentration of GOx (FAD), as shown in the following equation (7).

$$Glu\cos e + GOx\left(FAD\right) + O_2 \rightarrow Gluconolactone + GOx\left(FADH_2\right) \quad (7)$$

Based on the response of GOx/chitosan/TiO_2 nanorod/graphite microfiber electrode to glucose, the hybrid electrode can be used as a glucose biosensor. Figure S6 shows the CV of GOx/chitosan/TiO_2 nanorod/graphite microfiber electrode in pH 7.0 O_2-saturated PBS containing different concentrations of glucose. It can be seen that with the increase of glucose concentrations, the reduction current decreased correspondingly. The response principle of the hybrid electrode to glucose is shown in Scheme 1a.

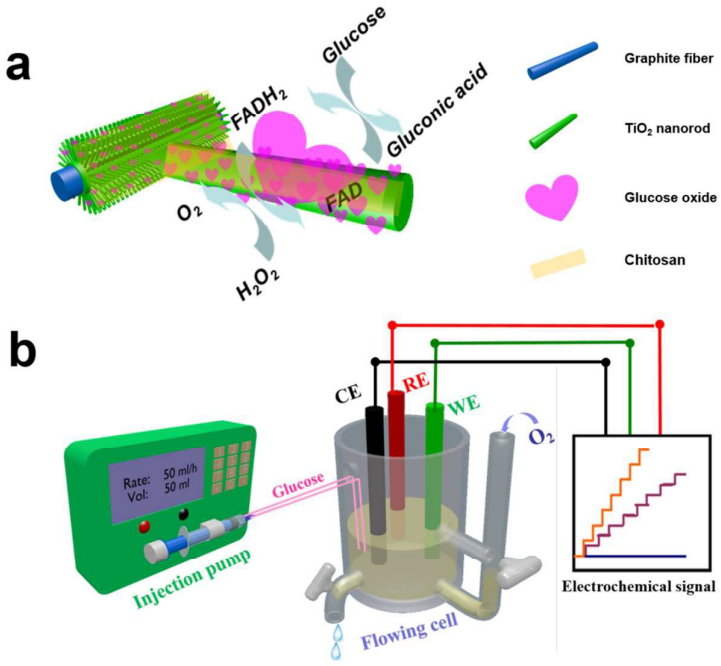

Scheme 1. (a) The response principle of the hybrid electrode to glucose. (b) Diagram of real-time detection of glucose in a flow system.

In order to simulate a flowing application scenario, the sensing performance of the GOx/chitosan/TiO_2 nanorod/graphite microfiber electrode was evaluated by amperometric measurement in a flowing system. The glucose solution was flowed into the electrolytic cell by controlling the rate of the injection pump, as shown in Scheme 1b.

View Article Online
DOI: 10.1039/C6NR01360K

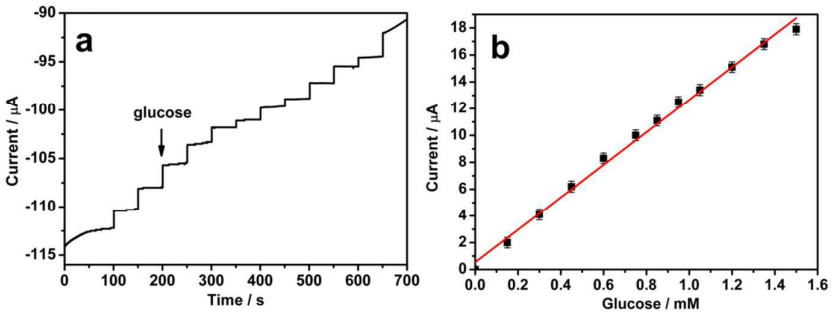

Figure 7. Amperometric response of GOx/chitosan/TiO_2 nanorod/graphite microfiber electrode on successive addition of glucose into 0.1 M pH 7.0 O_2-saturated PBS at an applied potential of -0.50V. (a) Calibration curve of GOx/chitosan/TiO_2 nanorod/graphite microfiber electrode for glucose (b).

To Figure 7a shows the typical current-time plots of the GOx/chitosan/TiO_2 nanorod/graphite microfiber electrode on successive injection of glucose into the O_2-saturated PBS solutions at -0.5V. This result demonstrates the fast response of the glucose sensor. The calibration curve obtained from the current-time plots shows a typical linear response with the increasing glucose concentration with a correlation coefficient of 0.995 (Figure 7b). The detection limit for GOx/chitosan/TiO_2 nanorod/graphite microfiber electrode was calculated to be 2.2μM at the signal-to-noise of 3 (S/N = 3). These results indicate that the developed glucose sensor have higher sensitivity, comparable to previously reported glucose biosensors. The comparison of analytical performance between GOx/chitosan/TiO_2 nanorod/ graphite microfiber and other modified electrodes have been listed in Table S1. Importantly, our hybrid microfibers can be expected to open opportunities in microelectrode or miniaturized electrochemical sensors.

The biosensor has good determination performance and widely applications mainly due to the excellent characteristics of the hybrid electrode. Vertically grown TiO_2 nanorods on microfibers have a lot of active sites and could promote the DET between the FAD and electrode surface. In addition, graphite microfiber has high conductivity, and the direct connection between the nanorods and the microfiber surface is conducive to the rapid transfer of electrons. Microfibers bundles are dispersed in the analytical solution could form a three dimensional electrode as a novel detection platform.

The apparent Michaelis-Menten constant km is calculated using the electrochemical version of the Line weaver – Burk equation (8).

$$\frac{1}{i_s} = \frac{k_m}{i_{\max}} \frac{1}{c} + \frac{1}{i_{\max}} \quad (8)$$

Here i_s is the steady-state current, i_{max} is the maximum current measured at the saturated substrate solution, and c is the glucose concentration. The k_m is determined to be 6.62mM, which is much lower than that of other types of enzyme electrodes.[17,50] This result indicates that the proposed hybrid electrode can remain superior enzymatic activity of GOx, which may be attributed to the nanostructure and biocompatibility of TiO_2.

The hybrid microfiber biosensor also exhibits excellent selectivity for glucose detection. Figure S7 showed the interferences in glucose detection using 0.5mM of ascorbic acid (AA), 0.5mM of dopamine (DA) and 0.5mM of uric acid (UA) at the applied potential of -0.50V. Upon addition of 0.5mM glucose in PBS, an obvious current response appeared. After successively injecting the AA, UA and DA into the solution, there is no significant change of the amperometric response. However, a significant current

View Article Online
DOI: 10.1039/C6NR01360K

response is observed for the subsequent addition of glucose, which demonstrates that the proposed biosensor has high selectivity for glucose.

In order to verify the practical application of the biosensor, GOx/chitosan/TiO_2 nanorod/graphite microfiber electrode was applied to the determination of glucose concentration in human serum samples from Jinan Central Hospital with a dilution step. As shown in Table S2, the values measured by the proposed biosensor were in good agreement with the standard value provided by the hospital, indicating that the proposed glucose biosensor has practical potential. The reproducibility and stability of the glucose biosensor were also been investigated, as shown in Figure S8. For the responses obtained by the 10 individual measurements of 100μM glucose, the relative standard deviation (RSD) of 3.3% was obtained, indicating that the GOx/chitosan/TiO_2 nanorod/graphite microfiber electrodes have good reproducibility. The GOx/chitosan/TiO_2 nanorod/graphite microfiber electrode was stored at 4°C when it is unused. The enzyme electrode can retained 96% of its initial current response over 15 days, demonstrating that the hybrid microfiber electrode is also stable for a long time to retain acceptable detection performance.

Conclusion

In this work, TiO_2 nanorods arrays were successfully in situ synthesized on graphite microfiber, and the obtained TiO_2 nanorod/graphite microfiber hybrid material was used as working electrode in a glucose biosensor. TiO_2 nanorods provide a large number of active sites for glucose molecules immobilization, and facilitate the DET of GOx at the surface of the hybrid microfibers electrode. The biosensor exhibits high sensitivity, high selectivity and excellent stability. In addition, the hybrid microfiber electrode has special one-dimensional morphology, small size and flexibility, and the bundle of microfibers can disperse in measurement system to from a 3 dimensional electrode, which further enhance the sensing property. The present study provides a feasible strategy for constructing on-time flowing glucose electrochemical biosensors using the fabricated 1D hybrid microfiber electrodes. Further development of this kind of biosensor may open substantial opportunities for the diagnosis and treatment of diabetes mellitus.

3. Experimental Section

3.1 Materials and Reagents

GOx (EC 1.1.3.4, 112U/mg, from Aspergillusniger) was supplied by Amresco. D-(+)-Glucose, chitosan and tetrabutyltitanate were purchased from Sigma-Aldrich. Graphite microfibers were purchased from Toray (Japan). All solutions were made up with twice-distilled water and all other chemicals were of analytical grade.

3.2 Preparation of TiO_2 nanorod/graphite hybrid microfiber and enzyme electrodes

The commercially available graphite microfibers were sonicated in acetone, 3.0M HNO3, 1.0M KOH and distilled water sequentially for a few minutes for surface cleaning before synthesis.[51] TiO_2 nanorods were in situ grown on graphite microfibers by a facile hydrothermal method. Briefly, the cleaned graphite microfibers were seeded by immersion in a mixed solution of tetrabutyltitanate (7ml), anhydrous ethanol (27ml) and diethanolamine (2ml) for 40min with ultrasound, followed by drying and thermal decomposition at 500℃ for 60min. For the hydrothermal synthesis, the seeded graphite microfibers were then put into Teflon-lined stainless steel autoclave, which contained a mixture of hydrochloric acid(14mL, 37wt%), ultrapure water (14mL) and titanium butoxide (0.5-1ml) at 150℃ for 10h. The producing microfibers were then rinsed with distilled water and ethanol, dried at 40℃ in

View Article Online
DOI: 10.1039/C6NR01360K

vacuum. TiO_2 nanorod/graphite microfibers were fixed on one side of a clean fluorine-doped tin oxide (FTO) glass and retain a length of microfibers as the electrode, while a copper wire which was used to connect the electrochemical workstation was fixed on the other side of the glass. Conductive silver adhesives were used to connect them and polydimethylsiloxane (PDMS) was used to encapsulate the FTO glass, as can be seen in Figure S9.

10mg of GOx was dispersed in 1.0 ml 0.5wt% chitosan solution and homogeneously mixed under gentle stirring for 60min. The TiO_2 nanorod/graphite microfiber electrodes were immersed into the mixed GOx/chitosan suspension for 30min, drying at 4℃ overnight. The GOx/chitosan/TiO_2 nanorod/graphite microfiber electrode was then obtained. The chitosan/graphite microfiber electrode, GOx/chitosan/graphite microfiber electrode and chitosan/TiO_2 nanorod/graphite microfiber electrode were prepared with the similar method.

3.3 Characterization

X-ray powder diffraction (XRD) patterns were recorded on an X-ray diffraction spectrometer (D8-advance, BrukerAXS, Germany). A field emission scanning electron microscope (FESEM) (HITACHI S8020, Japan) and transmission electron microscopy (TEM)(JEM 2100F, Japan) were used to characterize the morphology of the synthesized samples. A Fourier-transform infrared spectrum (FTIR) was collected using an IR spectrometer (NEXUS 670, America) over the range of 2500−500cm^{-1}.

3.4 Electrochemical measurements

Electrochemical measurements were performed with an electrochemical workstation (Gamry Reference 3000, America) with a standard three-electrode system. Ag/AgCl (saturated KCl) was used as reference electrode and a Pt plate (area, 1cm×1cm) was used as counter electrode. The as-prepared microfiber electrode was used as working electrode. The impedance spectra were measured in the frequency range from 0.1Hz to 100 kHz with voltage amplitude of 5mV. The electrical parameters of the system were fitted with a software package embedded in Gamry Reference 3000.

The microfiber immersed into the solution is 1cm. The electrochemical active surface area (ECSA) of GOx/chitosan/TiO_2nanorod/graphite microfiber electrode was calculated based on the Rundles–Service equation (9), assuming mass transport only by the diffusion process.[52,53]

$$I_p = 2.69\times10^5 AD^{1/2}n^{3/2}r^{1/2}C \quad (9)$$

Where n is the number of electrons participating in the reaction, D is the diffusion coefficient of the molecule ($6.7\pm0.02\times10^{-6}cm^2/s$), A is the electroactive surface area, C is the concentration of analyte (mol/cm^3), and r is the scan rate (V/s). The calculated ECSA of graphite microfiber, TiO_2 nanorod/graphite microfiber electrode and GOx/chitosan/TiO_2 nanorod/graphite microfibers electrode are about 0.8, 5.0 and 3.5 cm^2, respectively.

Supporting Information

Supporting Information is available from DOI: 10.1039/x0xx00000xor from the author.

Acknowledgments

The authors are thankful for funding from the National Natural Science Foundation of China (Grant No.51402063), China Postdoctoral Science Foundation (2014M550673), the fundamental research funds of Shandong University (2014QY003) and the “100 Talents Program” of the Chinese Academy of Sciences. Thanks for the support from the "Thousands Talents" program for pioneer researcher and his innovation team, China.

View Article Online
DOI: 10.1039/C6NR01360K

References

1 J. Wang, *Chem. Rev.*, 2008, **108**, 814–825.

2 V. Scognamiglio, *Biosens. Bioelectron*., 2013, **47**, 12–25.

3 G. Wang, X. Lu, T. Zhai, Y. Ling, H. Wang, Y. Tong and Y. Li, *Nanoscale*, 2012, **4**, 3123–3127.

4 A. Zhang, D. Wheeler, Y. Ling, G. Wang, X. Yang, B. Vilozny, B. Singaram, C. Gu and Y. Li, *Sci. Adv. Mater.*, 2012, **4**, 1–8.

5 P. R. Solanki, A. Kaushik, V. V. Agrawal and B. D. Malhotra, *NPG Asia Mater.*, 2011, **3**, 17–24.

6 V. Vamvakaki, K. Tsagaraki and N. Chaniotaki, *Anal. Chem*., 2006, **78**, 5538-5542.

7 J. Li, Z. Yang, Y. Tang, Y. Zhang and X. Hu, *Biosens. Bioelectron*., 2013, **41**, 698–703.

8 L. Meng, J. Jin, G. Yang, T. Lu, H. Zhang and C. Cai, *Anal. Chem*., 2009, **81**, 7271–7280.

9 P. Si, S. Ding, J. Yuan, X. W. Lou, D. H. Kim, *ACS Nano*, 2011, **5**, 7617–7626.

10 J. Tang, Y. Wang, J. Li, P. Da, J. Geng, G. Zheng, *J. Mater. Chem. A*, 2014, **2**, 6153-6157.

11 V. B. Kandimalla, V. S. Tripathi, H. Ju, *Biomaterials,* 2006, **27**, 1167–1174.

12 L. Zhang, W. Geng, S. Qiao, H. Zheng, G. Lu and Z. Yan, *ACS Appl. Mater. Interfaces*., 2010, **2**, 2767–2772.

13 S. Deng, G. Jian, J. Lei, Z. Hu and H. Ju, *Biosens. Bioelectron*., 2009, **25**, 373–377.

14 G. Liu, M. N. Paddon-Ro and J. J. Gooding, *Electrochem. Commun*., 2007, **9**, 2218–2223.

15 F. Jia, C. Shan, F. Li and L. Niu, *Biosens. Bioelectron*., 2008, **24**, 945–950.

16 B. R. Azamian, J. J. Davis, K.S. Coleman, C. B. Bagshaw and M. L. H. Green, *J. Am. Chem. Soc*., 2002, **124**, 12664–12665.

17 X. Kang, J. Wang, H. Wu, I. A. Aksay, J. Liu and Y. Lin, *Biosens. Bioelectron*., 2009, 25, 901–905.

18 S. Wu, Z. Zeng, Q. He, Z. Wang, S. Wang, Y. Du, Z. Yin, X. Sun, W. Chen and H. Zhang, *Small*, 2012, **8**, 2264–2270.

19 A. Salimia, E. Sharifi, A. Noorbakhsh and S. Soltanian, *Biosens. Bioelectron*., 2007, **22**, 3146–3153.

20 S. Bao, C. Li, J. Zang, X. Cui, Y. Qiao and J. Guo, *Adv. Funct. Mater*., 2008, **18**, 591–599.

21 S. Liu and A. Chen, *Langmuir*, 2005, **21**, 8409–8413.

22 E. Topoglidis, C. J. Campbell, A. E.G. Cass, and J. R. Durrant, *Langmuir*, 2001, **17**, 7899–7906.

23 J. Cui, D. Sun, S. Chen, W. Zhou, P. Hu, H. Liu and Z. Huang, *J. Mater. Chem*., 2011, **21**, 10633–10636.

24 K. N. Chappanda, Y. R. Smith, M. Misra, S. K. Mohanty, *Nanotechnology*, 2012, **23**, 1-8.

25 X. Wang, Y. Yan, B. Hao and G. Chen, *ACS Appl. Mater. Interfaces*, 2013, **5**, 3631–3637.

26 Z. Wang, H. Wang, B. Liu, W. Qiu, J. Zhang, S. Ran, H. Huang, J. Xu, H. Han, D. Chen, G. Shen, *ACS Nano*, 2011, **5**, 8412–8419.

27 F. C. P. F. Sales, R. M. Iost, M. V. A. Martins, M. C. Almeida and F. N. Crespilho, *Lab. Chip*., 2013, **13**, 468-474.

28 L. Xiang, P. Yu, M. Zhang, J. Hao, Y. Wang, L. Zhu, L. Dai and L.Mao, *Anal. Chem*., 2014, **86**, 5017–5023.

29 M. Kang, Y. Lee, H. Jung, J. H. Shim, N. S. Lee, J. M. Baik, S. C. Lee, C. Lee, Y. Lee and M. H. Kim, *Anal. Chem*., 2012, **84**, 9485-9491.

30 W. Guo, C. Xu, X. Wang, S. Wang, C. Pan, C. Lin and Z. Wang, *J. Am. Chem. Soc*., 2012, **134**, 4437–4441.

31 X. Cai, H. Wu, S. Hou, M. Peng, X. Yu and D. Zou, *Chem. Sus. Chem*., 2014, **7**, 474–482.

View Article Online
DOI: 10.1039/C6NR01360K

32 X. Yu, X. Han, Z. Zhao, J. Zhang, W. Guo, C. Pan, A. Li, H. Liu and Z. Wang, *Nano Energy*, 2014, **11**, 19–27.

33 Z. Sun, J.H. Kim, Y. Zhao, F. Bijarbooneh, V. Malgras, Y. Lee, Y. Kang and S. Dou, *J. Am. Chem. Soc*., 2011, **133**, 19314–19317.

34 S. Wu, H. Ju and Y. Liu, *Adv. Funct. Mater*., 2007, **17**, 585-592.

35 Y. Sang, Z. Zhao, J. Tian, P. Hao, H. Jiang, H. Liu and J. P. Claverie, *Small*, 2014, **10**, 3775–3782.

36 Q. Fan, D. Shan, H. Xue, Y. He, S. Cosnier, *Biosens. Bioelectron*., 2007, **22**, 816–821.

37 Z. Yang, Y. Tang, J. Li, Y. Zhang and X. Hu, *Biosens. Bioelectron*., 2014, **54**,528–533.

38 J. Lin, C. He, Y. Zhao and S. Zhang, *Sensor. Actuat. B-Chem*., 2009, **137**,768–773 .

39 C. Deng, J. Chen, X. Chen, C. Xiao, L. Nie and S. Yao, *Biosens. Bioelectron*., 2008, **23**, 1272–1277.

40 Z. Yang, X. Huang, R. Zhang, J. Li, Q. Xu and Xi. Hu, *Electrochim. Acta*., 2012, **70**, 325–330.

41 A. J. Bard and L. R. Faulkner, Electrochemical Methods: fundamentals and applications, *John Wiley& Sons, Inc., New York* , 2001, 228–242.

42 S. Liu and H. Ju, *Biosens. Bioelectron*., 2003, **19**, 177–183.

43 Y. Wu and S. Hu, *Bioelectrochemistry*, 2007, **70**, 335–341.

44 P. M. Schmidt, R. S. Brown and J. H.T. Luong, *Chem. Eng. Sci*., 1995, **50**, 1867–1876.

45 E. I. Iwuohaa, M. R. Smytha and M. E.G. Lyonsb, *J. Electroanal. Chem*., 1995, **390**, 35–45.

46 Z. Yang, Y. Ren, Y. Zhang, J. Li, H. Li, X. Huang, X. Hu and Q. Xu, *Biosens. Bioelectron*., 2011, **26**, 4337–4341.

47 S. Tang, X. Wang, J. Lei, Z. Hu, S. Deng, H. Ju, *Biosens. Bioelectron*., 2010, **26**, 432–436.

48 X. Xiao, M. Wang, H. Li and P. Si, *Talanta*, 2013,**116**, 1054–1059.

49 C. Li, Y. Liu, L. Li, Z. Du, S. Xu, M. Zhang, X. Yin and T. Wang, *Talanta*, 2008, **77**, 455–459.

50 C. Cai, M. Xu, S. Bao, C. Lei, D. Jia, *RSC Adv*., 2012, **2**, 8172–8178.

51 M. Zhang, K. Liu, L. Xiang, Y. Lin, L. Su and L. Mao, *Anal. Chem*., 2007, **79**, 6559–6565.

52 J. Du, R. Yue, F. Ren, Z. Yao, F. Jiang, P. Yang and Y. Du, *Biosens. Bioelectron*., 2014, **53**, 220–224.

53 J. Lu, I. Do, L. T. Drzal, R. M. Worden and I. Lee, *ACS Nano*, 2008, **2**, 1825–1832.

TOC:

View Article Online
DOI: 10.1039/C6NR01360K